Growth and properties of $Sr_{1-x}Ba_xBi_2TaNbO_9$ materials and thin films

M. S. TOMAR*, R. E. MELGAREJO
Physics Department, University of Puerto Rico, Mayaguez, PR 00681-9016
E-mail: m_tomar@feynman.upr.clu.edu

P. S. DOBAL, M. JAIN, R. S. KATIYAR
Physics Department, University of Puerto Rico, San Juan, PR 00931-3343

$Sr_{1-x}Ba_xBi_2TaNbO_9$ materials have been synthesized using a chemical solution route. Detailed x-ray diffraction and Raman spectroscopic studies indicates the formation of complete solid solutions for all compositions ($x = 0.0$ to 1.00) in $Sr_{1-x}Ba_xBi_2TaNbO_9$. Thin films were deposited by spin coating. Optical transmission of the film deposited on quartz disk showed the typical interference effect of optical thin films. Ferroelectric polarization on $Sr_{0.5}Ba_{05}Bi_2TaNbO_9$ film deposited on Pt substrate and annealed at $700\,^{\circ}C$, was measured to be $13.5\ \mu C/cm^2$. © *2001 Kluwer Academic Publishers*

1. Introduction

It is known that the barium ion is replaced by a strontium ion in the perovskite structure of $BaTiO_3$ to form a solid solution of $Ba_xSr_{1-x}TiO_3$ (BSTO). This material with a composition $x \approx 0.5$ is considered as one of the most promising dielectric materials for microwave frequencies. The Aurivillius phase materials [1, 2], consisting of alternating perovskite-like $A_{m-1}B_nO_{3m-1}$ and fluorite-like Bi_2O_3 layers where A is a mono-, di-, or trivalent cation, B is a cation with valence of 4 or 5, and m is the number of perovskite layers, are potentially important for ferroelectric and tunable dielectric devices. Important feature of this class of oxide materials is that A and B can be varied in order to understand the structure-property behavior. $SrBi_2Ta_2O_9$ (SBT) thin films have been expensively investigated due to their resistance to ferroelectric fatigue [3–5], but detailed characterization of $Sr_{1-x}Ba_xBi_2TaNbO_9$ has not been reported. We report here the synthesis, structural properties, and ferroelectric response of $Sr_{1-x}Ba_xBi_2TaNbO_9$.

2. Synthesis route

For the synthesis, reagent-grade chemicals of strontium hydroxide $[Sr(OH_2)\cdot 8H_2O]$, barium hydroxide $[Ba(OH_2)\cdot H_2O]$, bismuth acetate $[Bi(OOCCH_3)_3]$, niobium ethoxide $[Nb(OC_2H_5)_5]$, and tantalum ethoxide $[Ta(OC_2H_5)_5]$ were chosen as precursors for strontium, barium, bismuth, niobium and tantalum, respectively with methoxy ethanol $(C_3H_8O_2)$, 2-ethylhexanoic acid, and acetic acid as solvents. The stoichiometric ratios of the desired compositions were dissolved in proper volume ratios of the solvents. The solutions of the individual salts and ethoxides were mixed hot. This solution was dehydrated and then refluxed for about one hour.

Part of this clear solution was dried on a hot plate with constant stirring to make the powder. This powder was ground in agate crucible, and annealed at different temperatures to study the evolution of chemical reaction to form the compound. Another part of the solution was heated to make a bit denser solution for spin coating. X-ray diffraction, Raman scattering, optical spectroscopy, and ferroelectric probe were used for material characterization.

3. Results and discussion

3.1. X-ray diffraction studies

In order to investigate the evolution of chemical reaction with annealing temperature, we chose a fixed composition $Sr_{0.5}Ba_{0.5}Bi_2TaNbO_9$. X-ray diffraction patterns for the chemical conversion is shown in Fig. 1. It indicates that the reaction was completed at annealing temperature $\sim 700\,^{\circ}C$.

The powder samples of $Sr_{1-x}Ba_xBi_2TaNbO_9$, prepared with the compositions $x = 0.0, 0.1, 0.3, 0.5, 0.7, 0.9, 1.0$ and annealed at $700\,^{\circ}C$, were analyzed by x-ray diffraction (Cu K_α line). Fig. 2 shows the x-ray diffraction patterns for these compositions. It indicates that 2θ angles of $Sr_{1-x}Ba_xBi_2TaNbO_9$ peaks are not much different from that of SBT [6]. It also demonstrates that a complete solid solution is formed for all compositions, and x-ray reflections maintains the 2θ values as well as their relative intensities with Ba substitution, which is an indication that the Ba substitution is not random but is on Sr sites. Fig. 2 also shows that (006), (111) and (113) peaks develop systematically as Sr content increases in the compound, and these peaks are well developed for $SrBi_2TaNbO_9$ (with $x = 0.0$) and least developed for $BaBi_2TaNbO_9$ ($x = 1.0$). Since the ionic diameters of the Nb (0.74 Å) and Ta (68 Å) are close,

---

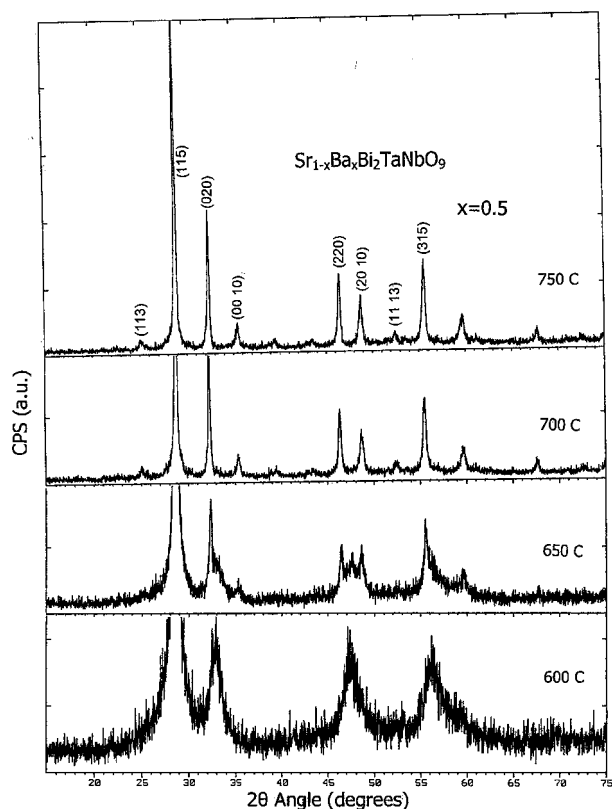*Author to whom all correspondence should be addressed.

Figure 1 X-ray diffraction patterns show the evolution of chemical reaction to form the compound $Sr_{0.5}Ba_{0.5}Bi_2TaNbO_9$.

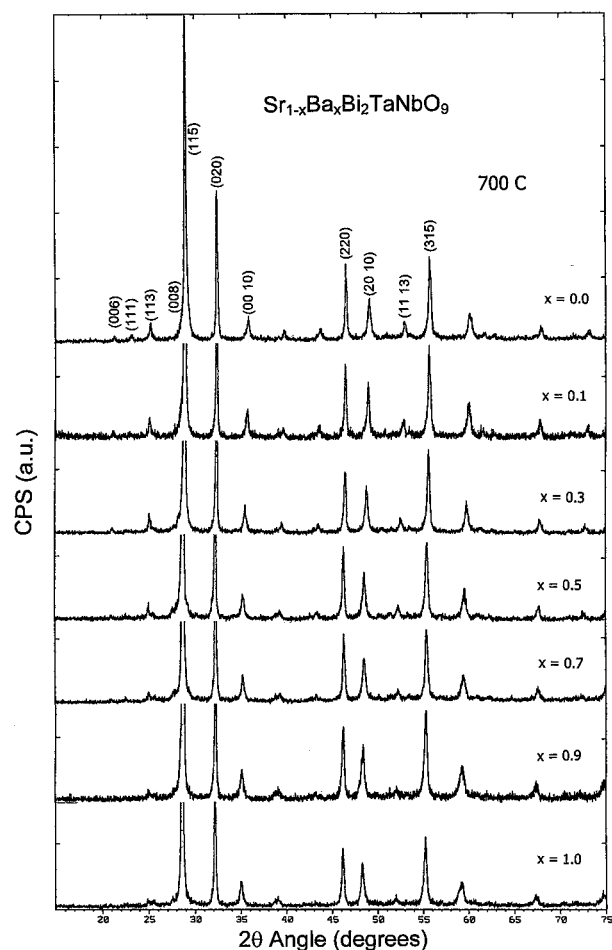*Figure 2* X-ray diffraction patterns of $Sr_{1-x}Ba_xBi_2TaNbO_9$ powder prepared by solution route for the compositions $x = 0.0$, 0.1, 0.3, 0.5, 0.7, 0.9, 1.0, and annealed at 700 °C.

their equal distribution on Ta sites of SBT does not show appreciable effect on 2θ angle and peak heights, if compared with the calculated and measured patterns of SBT [6].

3.2. Raman spectroscopic measurements

The Raman spectra were recorded using a spectroscopic apparatus (Model ISA T64000) from Jovin-Yvon France. 514.5 nm line of an argon ion laser from Coherent Inc was used as the excitation radiation. An optical microscopic was used to focus the laser on the sample and to collect the scattered signal. Scattered frequencies were analyzed with a triple monochromator and detected by a charge-coupled device (CCD) detection system. With 1800 grooves/mm gratings, each pixel of the CCD detector provides about $0.7\,cm^{-1}$ resolution in the spectral range used. Spectra were obtained from about 2 μm diameter circular area from the mixed samples at various different locations in the sample, chosen randomly. Identical spectra at different regions of each sample show that the material is homogeneous. The instrument was calibrated using the standard Si and CC14 samples before the Raman measurements.

The Aurivillius compound $Sr^{+2}Bi_2^{+3}Ta_2^{+5}O_9$ (SBT) consists of Bi_2O_2 layers and double perovskite type TaO_6 octahedral units. The divalent Sr atoms occupy the larger site of the $SrTaO_3$ type perovskite unit and have not been associated directly with any vibrational modes in SBT [7]. The crystal structures of SBT using electron and neutron diffraction techniques reveal orthorhombic distortions, which are also considered as distorted tetragonal structures [8–10]. In an approximate tetragonal structure SBT corresponds to I_4/mmm (D_{4h}^{17}) space group, which permits 12 Raman active modes [6, 7]. But, in the orthorhombic phase ($A2_1am$ space group) the factor group analysis leads to 81 zone center optical phonons [6]. However, all the Raman modes allowed in orthorhombic phases have not been observed in SBT or any other Aurivillius phases [11]. While B site substitution in SBT and its solid solutions with isostructural compounds have been studies [12, 13], few reports exist on the effect of A site substitution in this matearial [14]. Fig. 3 shows the room temperature Raman spectra of $Sr_{1-x}Ba_xBi_2TaNbO_9$ for different x values. Following the assignments of Graves *et al.* [7], the A_{1g} mode of SBT at about 813 cm^{-1}, which originates from TaO_6 octahedral vibrations along c axis shifts towards higher frequency in $SrBi_2TaNbO_9$ (SBTN) due to the lower reduced mass of Nb octahedra. Ba substitution in SBTN further shifts this mode to 840 cm^{-1}. The in-plane lattice parameters of orthorhombic/tetragonal unit cells in SBTN are small compared to the c parameters; the z-axis vibrations are expected to be very weakly affected by the change in ionic radius. Therefore, an increase in 813 cm^{-1} mode frequency could originate from the mass difference between Ba and Sr that greatly influences the environment around the TaO_6 octahedra. The 600 cm^{-1} E_g mode of SBT that shifts to 586 cm^{-1} in SBTN does not show any significant changes with Ba substitution. The low frequency Raman spectra of these materials are expanded in Fig. 4 for the clarity of the features. The most prominent effect of Ba substitution
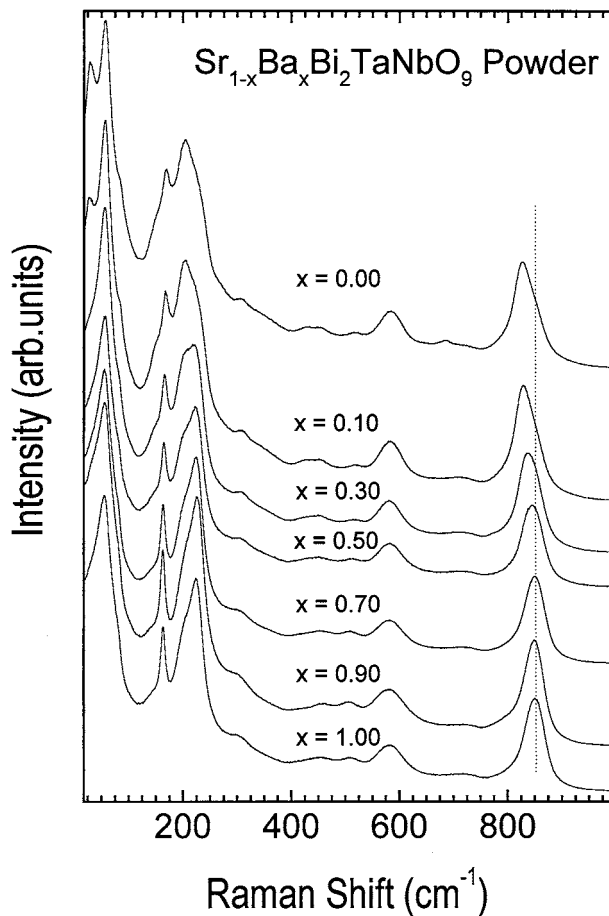
Figure 3 Room temperature Raman spectra of $Sr_{1-x}Ba_xBi_2TaNbO_9$ for $x = 0.0, 0.1, 0.3, 0.5, 0.7, 0.9, 1.0$, and annealed at 700 °C.
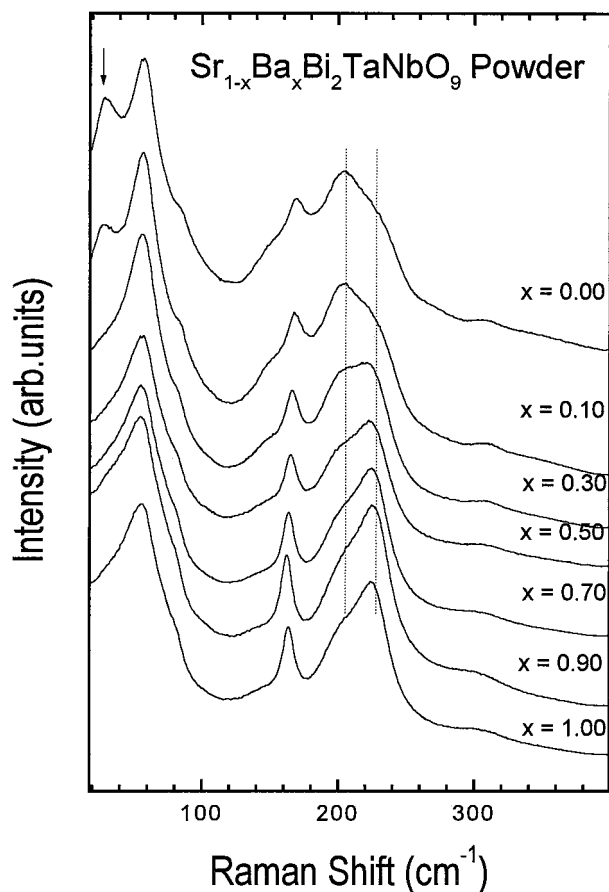

Figure 4 Low frequency Raman spectra of $Sr_{1-x}Ba_xBi_2TaNbO_9$ for different x values.

is on the SBT 25 cm^{-1} mode, which is marked by an arrow in Fig. 4. This mode has been regarded as a soft mode [15, 16] and relates to the lattice instability at the ferroelectric phase transition. In SBTN this mode disappears above 290 °C [17]. The transition temperature of SBT on the other hand decreases by 225 °C (from 335 to 110 °C) on replacing Sr by Ba [2]. The broadening and reduced intensity of the soft mode with increasing Ba content could be understood as an effect of the lowering transition temperature. Similar overdamped soft mode has also been observed in $BaBi_2Ta_2O_9$ [15]. Another effect of Ba substitution is the relative intensity changes of Bi_2O_2 vibrations along and perpendicular to c-axis at about 213 and 250 cm^{-1}, respectively in SBTN. These vibrational frequencies do not shift with Ba content. This indicates that the Bi_2O_2 layers are least affected by the compositional changes in the compound. But, their relative intensities change due to the possible change in local environment. In SBTN 213 cm^{-1} mode is relatively strong and as transition temperature decreases with increasing Ba in the compound, in plane vibrations about 250 cm^{-1} become more intense. All the low frequency Raman modes do not show any appreciable shifts in peak frequencies with Ba content. This shows that Ba substitution is taking place at the A sites and the material maintains the Auirvillius phase. The evolutions of $Sr_{0.5}Ba_{0.5}Bi_2TaNbO_9$ using Raman spectra with increasing annealing temperature are displayed in Fig. 5. These spectra reveal that though the
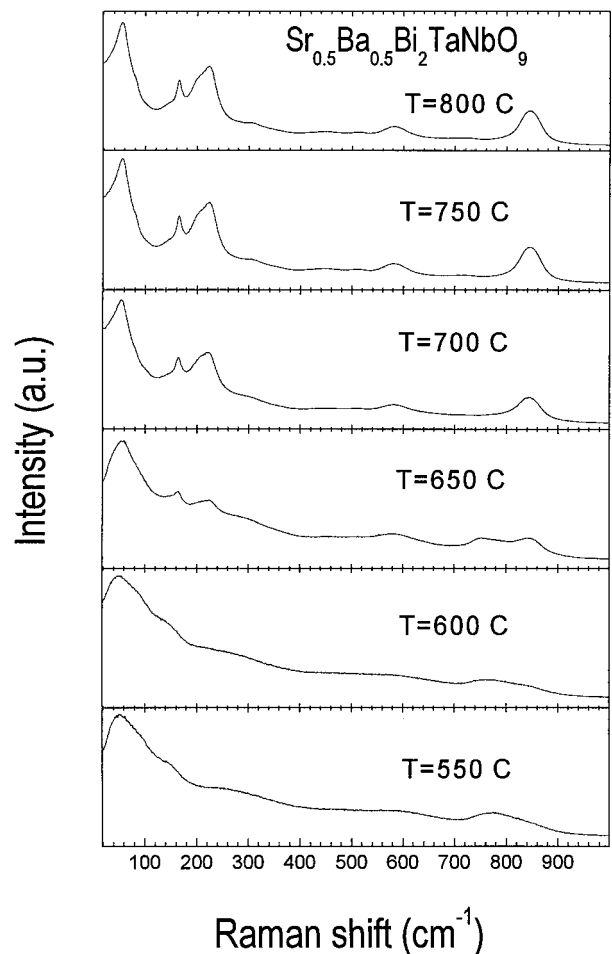

Figure 5 The evolution of $Sr_{0.5}Ba_{0.5}Bi_2TaNbO_9$ Raman spectra with increasing annealing temperatures in steps of 50 °C from 550 to 800 °C.
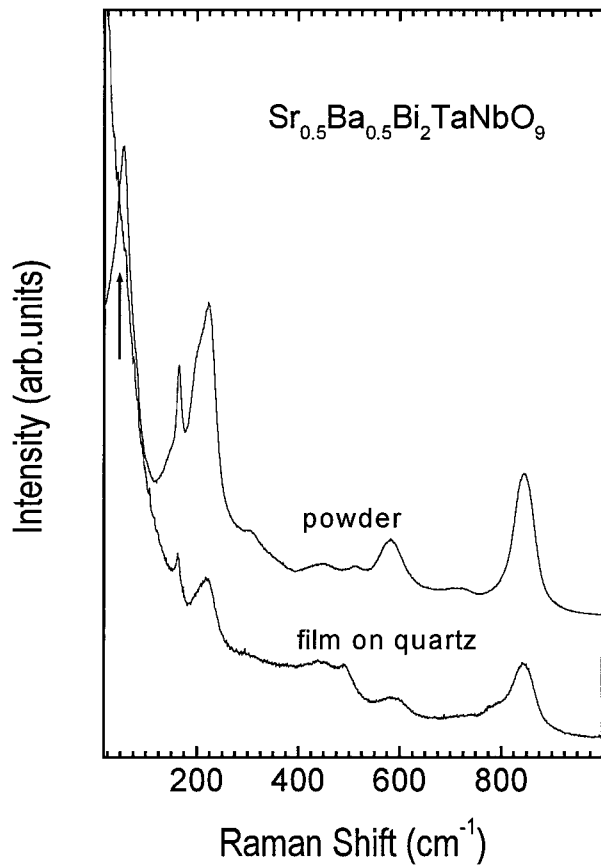
Figure 6 The comparison of $Sr_{0.5}Ba_{0.5}Bi_2TaNbO_9$ Raman spectra from powder and thin film on quartz.

Figure 7 Typical transmission curve for a thin $Sr_{0.5}Ba_{0.5}Bi_2TaNbO_9$ film on quartz substrate with uniform thickness of 860 nm.

Figure 8 Refractive index variation with excitation wavelength in $Sr_{0.5}Ba_{0.5}Bi_2TaNbO_9$ thin film.

crystallization begins at much lower temperatures, only at 700 °C or above the material crystallizes in an Aurivillius phase.

Thin films of $Sr_{0.5}Ba_{0.5}Bi_2TaNbO_9$ were deposited on quartz substrate by spin coating (Headway spinner) and annealed at 700 °C for 30 min. The Raman spectra of $Sr_{0.5}Ba_{0.5}Bi_2TaNbO_9$ powder and film are compared in Fig. 6. The identical Raman spectral features in thin film and powder indicate that the material quality remains excellent in thin films. However, relatively low intensity and broadening of the modes can be attributed to the smaller film thickness and interactions at the film substrate interface.

4. Optical and ferroelectric response

The characteristic feature of a weakly absorbing thin film on transparent substrate is to show interference effect in transmission spectrum. With a reference quartz disk, the transmission spectrum of $Sr_{0.5}Ba_{0.5}Bi_2TaNbO_9$ thin film on quartz was recorded. Fig. 7 shows the transmission curve with typical interfernce effect (maxima and minima). The interference effect also indicates that the film was uniformly deposited by spin coating. Thickness and refractive index of the film were calculated using the method described by Manifacier et al. [18] to determine the optical constants of a weakly absorbing thin film [19]. The refractive index of 860 nm thick $Sr_{0.5}Ba_{0.5}Bi_2TaNbO_9$ film is plotted (350–900 nm wavelength range) in Fig. 8, which shows that the refractive index decreases with increasing wavelength as expected.
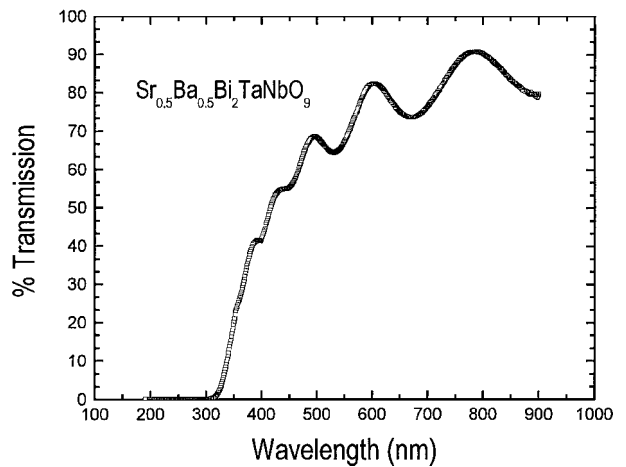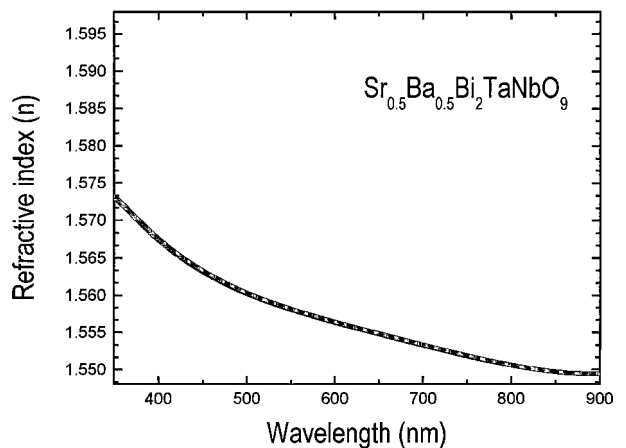
To study the ferroelectric effect, we deposited $Sr_{0.5}Ba_{0.5}Bi_2TaNbO_9$ film on Pt substrate and annealed at 700 °C for 30 min. The ferroelectric response was measured using RT 66A probe in a configuration Pt/$Sr_{0.5}Ba_{0.5}Bi_2TaNbO_9$ film/InGa top electrode. Ferroelectric response is shown in Fig. 9, with remnant polarization, $Pr \approx 13.5 \mu C/cm^2$ for the capacitor area
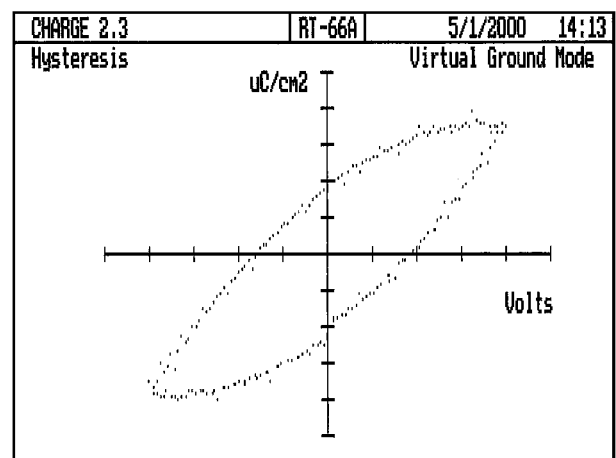

Figure 9 Ferroelectric response of $Sr_{0.5}Ba_{0.5}Bi_2TaNbO_9$ film on Pt substrate (Horizontal scale 1.5 V/Div., Vertical scale: 7 $(\mu C/cm^2)$/Div.).

of 0.25 cm^2. This is an improvement in Pr value over $SrBi_2Ta_{0.8}Nb_{1.2}O_9$ film [4] prepared by pulsed laser deposition (PLD), but the films seem to be leaky.

5. Conclusion

We reported a chemical solution route for the synthesis of $Sr_{1-x}Ba_xBi_2TaNbO_9$ powders and thin films with their structural studies using x-ray diffraction and Raman spectroscopy. $Sr_{0.5}Ba_{0.5}Bi_2TaNbO_9$ film showed ferroelectric response. This material could have tunable dielectric properties in microwave frequencies.

Acknowledgements

References

1. B. AURIVILLIUS, *Arkiv. Kemi* **1** (1949) 463.
2. E. C. SUBBARAO, *J. Phys. Chem. Solids* **23** (1962) 665.
3. C. A. PAZ DE ARAUJO, J. D. CUCHIARO, L. D. MCMILLAN, M. C. SCOTT and J. F. SCOTT, *Nature* **374** (1995) 627.
4. S. B. DESU and D. P. VIJAY, *Mater. Sci. and Engn. B* **32** (1995) 83.
5. O. AUCIELLO, C. M. FOSTER and R. RAMESH, *Annu. Rev. Mater. Sci.* **28** (1998) 501.
6. M. P. MORET, R. ZALLEN, R. E. NEWNHAM, P. C. JOSHI and S. B. DESU, *Phys. Rev. B* **57** (1998) 5715.
7. P. R. GRAVES, G. HUA, S. MYHRA and J. G. THOMPSON, *J. Solid. State Chem.* **144** (1995) 112.
8. R. E. NEWNHAM, R. W. WOLFE, R. S. HORSEY, F. A. DIAZ-COLON and M. I. KAY, *Mat. Res. Bull.* **8** (1973) 1183.
9. A. D. RAE, J. G. THOMPSON and R. L. WITHERS, *Acta. Cryst. B* **48** (1992) 418.
10. Y. SHIMAKAWA, Y. KUBO, Y. NAKAGAWA, T. KAMIYAMA, H. ASANO and F. IZUMI, *Appl. Phys. Lett.* **74** (1999) 1904.
11. R. MELGAREJO, M. S. TOMAR, P. S. DOBAL and R. S. KATIYAR, *J. Mater. Res.* **8** (August 2000)
12. X. ZHANG, P. GU and S. B. DESU, *Phys. Stat. Sol. (a)* **160** (1997) 35.
13. S. O. RYU, S. TIRUMALA, P. C. JOSHI and S. B. DESU, Thin Solid Films **340** (1999) 53.
14. C.-H. LU and J.-H. BAI, *Int. Ferroelectrics* **26** (1999) 57.
15. S. KOJIMA, *J. Phys.: Condens. Matter* **10** (1998) L327.
16. J. LIU, G. ZOU, H. YANG and Q. CUI, *Solid State Commun.* **90** (1994) 365.
17. S. KOJIMA, I. SAITOH and T. YAMAMOTO, in Proceedings of 11th IEEE International Symposium on Application of Ferroelectrics, Montreux, Switzerland, IEEE catalog No. 98CH36245, 1998, p. 471.
18. J. C. MANIFACIER, J. GASIOT and J. P. FILLARD, *J. Phys. E: Sci. Instrum.* **9** (1976) 1002.
19. S. B. MAJUMDAR, Y. N. MOHAPATRA and D. C. AGRAWAL, *J. Mater. Sci.* **32** (1997) 2141.